DMD Fast Forward. Published on August 20, 2007 as doi:10.1124/dmd.107.017723

P-glycoprotein-mediated Active Efflux of the Anti-HIV1 Nucleoside Abacavir Limits Cellular Accumulation and Brain Distribution

Naveed Shaik, Nagdeep Giri, Guoyu Pan and William F. Elmquist

Department of Pharmaceutics, College of Pharmacy, University of Minnesota,
308 Harvard St. SE, Minneapolis, MN 55455.

Department of Pharmaceutics (N.S., N.G., G.P. and W.F.E)

Running Title:

P-gp mediated efflux of abacavir

Address correspondence to: William F. Elmquist, Ph.D.

Department of Pharmaceutics, University of Minnesota

308 Harvard St. SE

Room 9-125, Weaver-Densford Hall

Minneapolis, MN 55455

U.S.A

Tel: 1-612-625-0097

Fax: 1-612-626-2125

Email: elmqu011@umn.edu

The number of text pages: 21

The number of tables: 1

The number of figures: 11

The number of references: 37

The number of words in Abstract: 250

The number of words in Introduction: 651

The number of words in Discussion: 1837

Abbreviations: HIVE, human immunodeficiency virus encephalopathy; CNS, central nervous system; ART, active retroviral therapy; P-gp, P-glycoprotein; ABC, ATP Binding Cassette; PI, protease inhibitor; NRTI, nucleoside reverse transcriptase inhibitor; AUC, area under the concentration-time curve; HPLC, high performance liquid chromatography; BBB, blood-brain barrier; BCA, bicinchoninic acid; ER, efflux ratio

Abstract:

P-glycoprotein (P-gp) mediated efflux at the blood-brain barrier has been implicated in limiting the brain distribution of many anti-HIV1 drugs, primarily protease inhibitors, resulting in sub-optimal concentrations in this important sanctuary site. The objective of this study was to characterize the interaction of abacavir with P-gp and determine if P-gp is an important mechanism in limiting abacavir delivery to the CNS. In-vitro and in-vivo techniques were employed to characterize this interaction. Abacavir stimulated P-gp ATPase activity at high concentrations. The cellular accumulation of abacavir was significantly decreased by ~70% in MDCKII-MDR1 monolayers compared to wild-type cells and was completely restored by the P-gp inhibitors LY335979 and GF120918. Directional flux experiments indicated that abacavir had greater permeability in the basolateral-to-apical (B-to-A) direction (1.58E-05 cm/s) than in the apical-to-basolateral (A-to-B) direction (3.44E-06 cm/s) in MDR1-transfected monolayers. The directionality in net flux was abolished by both LY335979 and GF120918. *In-vivo* brain distribution studies showed that the AUC_{plasma} in mdr1a (-/-) CF-1 mutant mice was ~2-fold greater than AUC_{plasma} in the wild-type, while the AUC_{brain} in the mutant was 20-fold higher than wild-type. Therefore, the CNS drug targeting index (DTI), defined as the ratio of AUC brain-to-plasma for mutant over wild-type, was greater than 10. These data are the first *in-vitro* and *in-vivo* evidence that a nucleoside reverse transcriptase inhibitor is a P-gp substrate. The remarkable increase in abacavir brain distribution in P-gp deficient mutant mice over wild-type suggests that P-gp may play a significant role in restricting the abacavir distribution to the CNS.

DMD Fast Forward. Published on August 20, 2007 as DOI: 10.1124/dmd.107.017723
This article has not been copyedited and formatted. The final version may differ from this version.

Introduction

Abacavir, a carbocyclic nucleoside and a guanosine analog, is a member of the nucleoside reverse transcriptase (NRTI) family of anti-HIV1 agents. Abacavir is metabolized intracellularly to its active form, carbovir triphosphate (Daluge et al., 1997). Abacavir is used in combination with other NRTIs as well as protease inhibitors in active retroviral therapy (ART) (Josephson et al., 2007).

HIV1 can infect the CNS at a very early stage of the disease and can lead to the development of AIDS dementia complex (Ances and Ellis, 2007). The CNS has been cited as a reservoir for the HIV1 virus due to incomplete suppression of the viral replication (Kerza-Kwiatecki and Amini, 1999). Sub-optimal concentrations of anti-HIV1 drugs in the CNS can not only lead to incomplete eradication of the virus but also provide ideal conditions for the selection of more virulent mutants (Lipniacki, 2003). Recent reports have highlighted the compartmentalization and independent evolution of primary, as well as, secondary drug resistant viral mutations in the CNS as a response to inadequate concentrations of both reverse transcriptase and protease inhibitors (Smit et al., 2004).

The CNS penetration of a number of anti-HIV1 drugs used in ART is limited (Langford et al., 2006). One of the factors implicated in limiting the CNS distribution of anti-retroviral drugs is the action of drug efflux transporters. These are transmembrane proteins belonging to the ABC (ATP Binding Cassette) superfamily that utilize the energy generated from ATP hydrolysis to transport drugs against a concentration gradient. P-glycoprotein (P-gp), a member of this superfamily, has been implicated in conferring resistance against a variety of drugs (Fromm,

2003). It is highly expressed on the luminal surface of the brain microvasculature that forms the blood-brain barrier (BBB) (Cordon-Cardo et al., 1989). P-gp has been shown to modulate the brain distribution of most HIV protease inhibitors (Kim et al., 1998). Inhibition of P-gp at the BBB (Choo et al., 2000), as well as the use of transgenic mouse models lacking P-gp (Kim et al., 1998; Choo et al., 2000) has lead to enhanced brain penetration and distribution of protease inhibitors. This highlights the role of P-gp in limiting this class of anti-HIV1 drug distribution to the CNS. Recently, the breast cancer resistance protein (Bcrp1), another member of the ABC superfamily (ABCG2), has been shown to actively efflux nucleoside reverse transcriptase inhibitors (Pan et al., 2007). Similar to P-gp, Bcrp1 is localized on the luminal surface of the BBB, is instrumental in the efflux of drugs and shares common substrates with P-gp. Bcrp1 has been shown to efflux the NRTIs, AZT and 3TC (Wang et al., 2003; Pan et al., 2007) and abacavir (Pan et al., 2007).

The CNS penetration of abacavir has been shown in many animal models to be similar to AZT (zidovudine) (Daluge et al., 1997). *In situ* brain perfusion studies in guinea pig showed nonlinear uptake of ABC into the brain, raising the possibility that a saturable efflux process could be influencing abacavir brain distribution (Thomas et al., 2001). Recent transport competition studies have examined the inhibitory activity of abacavir on both P-gp and Bcrp1. It was found that among all the NRTIs tested, abacavir was the only NRTI that inhibited P-gp-mediated transport in a calcein uptake assay (Storch et al., 2007). Moreover, abacavir and AZT moderately influenced Bcrp1-mediated transport of pheophorbide A, a prototypical Bcrp1 substrate (Weiss et al., 2007).

The goal of this study was to investigate possible mechanisms that may limit the CNS distribution of abacavir. One of these mechanisms could be an efflux transporter, such a P-gp. Therefore, the specific objective was to examine the interaction of abacavir with P-gp using biochemical assays, *in vitro* cell transport and *in vivo* brain distribution studies.

Material and Methods:

Chemicals

[^{3}H]- Vinblastine sulfate, [^{3}H]-abacavir and [^{14}C]-AZT were obtained from Moravek Biochemicals (Brea, CA). Verapamil was obtained from the Sigma Chemical Co. (St.Louis, MO). GF120918 (N-[4-[2-(6, 7-dimethoxy-3,4-dihydro-1H-isoquinolin-2-yl)ethyl]phenyl]-5-methoxy-9-oxo-10H-acridine-4-carboxamide) was a gift from GlaxoSmithKline (Research Triangle, NC). Fumitremorgin C (FTC; (9'R-(9'alpha(4S*(R*)),9'abeta))-4-(2-(1-(Acetyloxy)-2-methylpropyl)-4-oxo-3(4H)-quinazolinyl)-1',3,4,9'a-tetrahydro-1'-hydroxy-2',2'-dimethylspiro(furan-2(5H),9'-(9H)imidazo(1,2-a) indole)-3',5(2'H)-dione) was obtained from the NCI, Ko143 (a fumitremorgin C analog) (Allen et al., 2002) was kindly provided by Dr. Alfred Schinkel (NCI, Netherlands) and LY335979 ((R)-4-((1aR,6R,10bS)-1,2-Difluoro-1,1a,6,10b-tetrahydrodibenzo(a,e)cyclopropa(c)cycloheptan-6-yl)-alpha-((5-quinoloyloxy)methyl)-1-piperazineethanol, trihydrochloride) was a gift from Eli Lilly and Co. (Indianapolis, IN). Human P-gp expressing membranes were purchased from BD Biosciences (San Jose, CA). All other chemicals used were HPLC or reagent grade.

Cell lines

Wild-type (WT) and MDR1-transfected epithelial Madin-Darby canine kidney (MDCKII) cells were obtained from Dr. Piet Borst (The Netherlands Cancer Institute, Amsterdam, The Netherlands) and maintained in Dulbecco's modified eagle medium (Mediatech, Inc., Herndon, VA) fortified with 10% heat deactivated fetal bovine serum (SeraCare Life Sciences, Inc., Oceanside, CA), 100 U/mL of penicillin and 100 µg/mL of streptomycin (Sigma Aldrich, St.Louis, MO) at 37°C under humidity and 5% CO_2 tension. The MDCKII-MDR1 cell growth media additionally contained 80 ng/mL of colchicine to maintain positive selection pressure for P-gp expression. Cells between passages 5 and 15 were used in all experiments.

Animals

Age matched wild-type CF1 (*Crl: CF1*) and naturally mutant CF1 (*mdr1a (-/-)*) mice *(Crl: CF1-Abcb1a*), lacking the mdr1a gene, were purchased from Charles River Laboratories (Wilmington, MA). All the mice were male and between 9 and 12 weeks old. Animals were maintained under temperature-controlled conditions with a 12h light/dark cycle and unlimited access to food and water. All studies were conducted according to the guidelines set by the *Principles of Laboratory Animal Care* (National Institute of Health) and were approved by The Institutional Animal Care and Use Committee of the University of Minnesota.

P-gp ATPase assay

P-gp ATPase activity was evaluated using a suspension of human P-gp over expressing membranes obtained from baculovirus-infected insect cells (High Five, BTI-TN5B1-4) in TMEP

buffer. Briefly, a suspension of P-gp over-expressing membranes was incubated at 37°C for 20 min in the presence of 4mM ATP with and without 100, 200 and 500 µM abacavir. An identical reaction mixture containing 100 µM sodium orthovanadate was assayed in parallel. Orthovanadate inhibits P-gp by trapping Mg2+ADP in the nucleotide-binding site. Thus, the ATPase activity measured in the presence of orthovanadate represents non P-gp ATPase activity and was subtracted from the total activity measured in the non-orthovanadate treated case to yield the P-gp mediated ATPase activity. The reaction was stopped by the addition of 10% SDS and the liberated inorganic phosphate was detected by a colorimetric reaction of inorganic phosphate with a solution of ascorbic acid and ammonium molybdate at 650 nm. The nanomoles of phosphate released were determined from the absorbance values, using a standard curve generated from inorganic potassium phosphate standards (0-60 nM range). The same procedure was followed for control membranes (also obtained from BD Biosciences) that do not express P-gp. Verapamil (20µM) was used as a positive control for P-gp ATPase stimulatory activity.

Cellular accumulation studies in MDCKII cells

For the accumulation experiments, cells were seeded in clear polyester 12-well plates (TPP© cell culture plate) at a seeding density of $2x10^5$ cells/well. The media was changed every other day and the cells formed confluent monolayers in 4 days. On the day of the experiment, the media was aspirated and the confluent monolayer was washed twice with pre-warmed (37°C) assay buffer. The cells were pre-incubated for 30 mins with 1 mL of assay buffer, after which the buffer was aspirated and the cells were exposed to a tracer solution of radiolabelled drug in 1 mL assay buffer per well. The plates were continuously agitated at 60 rpm in an orbital shaker and maintained at 37°C for the duration of the experiment. Following a 3-hour accumulation period

the supernatant was aspirated and the cells were first washed three times with 2 mL of ice cold phosphate buffered saline (PBS) and then solubilized using 1mL of mammalian protein extraction reagent (MPER; Pierce Biotechnology, Inc., Rockford, IL). A 200µL sample was drawn from each well in triplicate and 4 mL of scintillation fluid (ScintiSafe Econo1 cocktail; Fisher Scientific Co.) was added to each sample and counted using liquid scintillation counting (LS-6500, Beckman Coulter, Inc., Fullerton, CA) to determine the radioactivity associated with the cells. The protein concentration was determined using the BCA protein assay (Pierce Biotechnology, Inc., Rockford, IL) to normalize the radioactivity in each well.

For inhibition studies, the cells were treated with the inhibitor (1µM LY335979 or 5µM GF120918 for P-gp; 200 nM Ko143 or 10 µM FTC for Bcrp1) both during the pre-incubation and the accumulation periods. Drug accumulation in WT and MDR1 cells was expressed as a percentage of the control radioactivity measured in the wild-type cells (DPM) per milligram of protein. The stock solutions for all the inhibitors used were prepared in DMSO and diluted using assay buffer (NaCl, 122 mM; $NaHCO_3$, 25 mM; Glucose, 10 mM; HEPES, 10 mM; KCl, 3 mM; $MgSO_4 \cdot 7H_20$, 1.2 mM; $CaCl_2 \cdot H_20$, 1.4 mM; K_2HPO_4, 0.4 mM; pH of 7.4) to obtain working solutions such that the final concentration of DMSO was less than 0.1%.

Directional flux across MDCKII cell monolayers

The method used in this study was similar to that previously described by Dai et al. (Dai et al., 2003). Briefly, MDCKII WT or MDR1 cells were seeded at a density of $2x10^5$ cells/well on

semi-permeable membrane supports in six-well transwells (Corning Inc., Corning, NY). The media was changed every day and the cells formed confluent polarized epithelial monolayers in 4 days. The trans-epithelial electrical resistance (TEER) was 300 ± 8 Ohm*cm^2 in the MDCKII WT monolayers and 275 ± 26 Ohm*cm^2 in the MDCKII MDR1 transfected monolayers. Mannitol flux across the monolayer was also measured to confirm the existence of tight junctions with approximately 1% per hour flux. The monolayers were washed with pre-warmed (37°C) assay buffer and, following a 30 min pre-incubation, a tracer solution of radiolabelled drug in assay buffer was added to the donor side (apical side; 1.5mL, basolateral side; 2.6mL). Fresh assay buffer was added to the receiver side and a 100µL of the receiver compartment was sampled at 0, 10, 20, 30, 45, 60 and 90 mins. The volume sampled was immediately replaced with fresh assay buffer. Additional samples were drawn at 0 and 90 mins in the donor compartment. The amount of radioactivity in the samples was determined using liquid scintillation counting. The apical-to-basolateral (A-to-B) flux was determined by addition of radiolabelled drug solution to the apical compartment and sampling the basolateral compartment, while for basolateral-to-apical (B-to-A) flux, the donor was the basolateral compartment and the apical compartment was sampled over time.

When an inhibitor was used in the flux study, the cell monolayers were pre-incubated with the inhibitor (1µM LY335979 or 5µM GF120918 for P-gp and 200 nM Ko143 for Bcrp1) for 30 min followed by determination of the A-to-B and the B-to-A flux with the inhibitor being present in both compartments throughout the course of the experiment.

DMD Fast Forward. Published on August 20, 2007 as DOI: 10.1124/dmd.107.017723
This article has not been copyedited and formatted. The final version may differ from this version.

Permeability calculation

The effective permeability (P_{eff}) was calculated by the following equation,

$$Peff = \frac{(dQ/dt)}{A*Co} \qquad \text{Equation 1,}$$

where Q is the amount of radioactivity transported across the monolayer, t is time, dQ/dt is the mass transport rate, A is the effective surface area of the cell monolayer and C_o is the initial donor concentration. The efflux ratio (ER) was used as a measure of P-gp mediated efflux and calculated as the P_{eff} in the B-to-A direction over P_{eff} in the A-to-B direction.

LY335979 dose dependence study

Directional flux experiments for abacavir in the B-to-A direction across the MDCKII-MDR1 monolayers were conducted in the presence of varying concentrations of the P-gp inhibitor LY335979. The experimental procedure used was the same as described in the previous section. The B-to-A flux of abacavir was determined in the presence of 0, 0.015, 0.03, 0.06, 0.125, 0.25, 0.5 and 1 μM LY335979. The inhibitory sigmoid E_{max} model with baseline (equation 2) was employed to fit the model to the data using the following equation,

$$E = E_0 - \frac{I_{\max} * C^{\gamma}}{IC_{50}^{\gamma} + C^{\gamma}} \qquad \text{Equation 2,}$$

DMD Fast Forward. Published on August 20, 2007 as DOI: 10.1124/dmd.107.017723
This article has not been copyedited and formatted. The final version may differ from this version.

where E is the B-to-A permeability of abacavir, E_0 is the permeability of abacavir when no inhibitor is present, I_{max} is the maximal inhibition of abacavir B-to-A permeability by LY335979, IC_{50} is the concentration of LY335979 that shows half-maximal inhibition, C is the concentration of LY335979 and γ is the shape factor.

Brain distribution of abacavir in mdr1a (-/-) deficient and wild-type CF1 mice

All mice were allowed to acclimatize for a minimum of 5 days upon arrival. Ziagen® oral solution (abacavir sulfate, 20 mg/mL) diluted with normal saline to 5mg/mL was administered to the mice at a dose of 10 mg/kg via tail vein injection. The animals were euthanized using a CO_2 chamber at pre-determined time points postdose (5, 10, 20, 30 and 40 mins, n=6 for each time point). Blood was collected by cardiac puncture and transferred to heparinized tubes. Plasma was isolated from the blood by centrifugation at 3000 rpm for 10 mins at 4°C. Whole brain was immediately removed from the skull, washed in ice cold PBS to remove extraneous blood and flash-frozen in liquid nitrogen. All samples were stored at -80°C until further analysis by HPLC.

Determination of abacavir concentrations in plasma and brain homogenate by HPLC

On the day of analysis, the brain samples were homogenized on ice in 3 volumes of 5% BSA in phosphate buffered saline using a dounce homogenizer (7mL; Kontes, Vineland, NJ). The plasma and brain homogenate samples were analyzed using separate standard curves for each matrix. For plasma, 100 µl samples were spiked with 100 ng of AZT (3'-azido-3'-deoxythymidine) as the internal standard. Plasma samples were extracted by liquid-liquid extraction using 8 parts of ethyl acetate and one part of sample with vigorous vortexing for 5 minutes. The mixture was then centrifuged for 10 min at 14,000 rpm at room temperature and

the resultant supernatant was dried under a gentle flow of nitrogen (N-Evap, Organomation Associates, Berlin, MA), reconstituted in 100 µl of mobile phase, and then 30 µl was injected onto the HPLC system. For brain, 500 µl of homogenate was spiked with 50 ng of AZT and sample preparation was then similar to that of plasma. The analysis was performed on a Hypersil-BDS column (C-18, 2.1mm x 150mm, 5µm; Keystone Scientific, Inc.) maintained at 40ºC using a Shimadzu column oven (CTO-10Avp). The HPLC system consisted of a Shimadzu pump (LC-10ATvp), flow control valve (FCV-10ALvp), degasser (DGU-20A5), auto injector (SIL-10ADvp), system controller (SCL-10Avp) and detector (SPD-10Avp). The mobile phase consisted of 50 mM ammonium phosphate and 50 mM sodium citrate buffer (pH 6.5), acetonitrile and methanol (89:10:1) at a flow rate of 0.25 ml/min and UV absorbance was measured at 285 nm. The plasma and brain concentrations are reported as ng/ml and ng/gm brain tissue, respectively.

Pharmacokinetic analysis:

Non-compartmental analysis (WinNonlin 5.0.1; Mountain View, CA) was employed to obtain pharmacokinetic parameters from concentration-time data in plasma and brain. The terminal rate constants for plasma and brain were determined from the last three data points of the respective concentration-time profiles. The areas-under the concentration-time profiles for plasma (AUC_{plasma}) and brain (AUC_{brain}) from time zero to infinity were calculated using the trapezoidal method with estimation of the AUC from the last measured time point to infinity accomplished by dividing the last measured concentration by the respective terminal rate constant. In case of plasma, the AUC from time zero to the first measured time point was obtained by back-extrapolation of the first two data points to the concentration estimated at time zero. The

DMD Fast Forward. Published on August 20, 2007 as DOI: 10.1124/dmd.107.017723
This article has not been copyedited and formatted. The final version may differ from this version.

enhancement in brain exposure of abacavir in the P-gp deficient mice compared to wild-type mice was represented by the drug targeting index (DTI), calculated as,

$$DTI = \frac{(AUC_{brain} / AUC_{plasma})_{mutant}}{(AUC_{brain} / AUC_{plasma})_{wild-type}}$$

Equation 3,

Statistical analysis:

Statistical analysis was conducted using SigmaStat, version 3.1(SYSTAT Software, Inc.). Groups were compared by one-way ANOVA with Holm-Sidak post-hoc test for multiple comparisons at a significance level of $p<0.01$. When groups failed the normality or equal variance test, ANOVA on ranks with the Tukey post-hoc test was used for multiple comparisons. The brain-to-plasma concentration ratios between wild-type and mutant CF-1 mice were compared using the non –parametric Mann-Whitney rank sum test. Due to the inability of obtaining concentrations at multiple time points from a single mouse, destructive sampling was used. A total of six mice were used at each time point to estimate the inter-animal variability and the area under the curve was constructed from the mean plasma concentration at each time point. The variance of the AUC was estimated using the method described by Yuan (Yuan, 1993). This method allows for the determination of the variability in the AUC estimate from the variability about the mean concentration at each time point, assuming the mean at each time point is independent and the terminal rate constant is the same for each animal. It is reasonable to assume that the sample means are independent of each other and given that the coefficient of

variation in the terminal phase of the curve is low, this method was used to statistically compare AUCs. The AUCs were statistically compared using the z-test at a significance level of $p<0.05$.

Results:

P-gp ATPase assay

Verapamil (20 µM) significantly stimulated the P-gp ATPase activity over control ($p<0.01$) as shown in Figure 2. The test compound abacavir, showed an increase in the ATPase assay at 100, 200 and 500 µM, but due to the high variability in the data, statistically significant stimulation of P-gp ATPase activity was seen only at 500 µM ($p<0.01$, Figure 2).

Cellular accumulation studies in the MDCKII cells

[^{3}H]-vinblastine was used as a positive control to verify P-gp function in the cell accumulation assays. As seen in figure 3, [^{3}H]-vinblastine had a significantly lower accumulation ($p<0.001$) in the MDR1 cells compared to wild-type cells. [^{3}H]-abacavir accumulation in the MDR1 transfects was significantly lower (~70%; $p<0.001$) than in the wild-type cells (expressed as 100%), while the accumulation of [^{3}H]-AZT was not significantly different between the two cell types. Treatment with the P-gp inhibitors LY335979 (1µM) and GF120918 (5µM) completely abolished the efflux action of P-gp ($p<0.001$, compared to MDR1 control) resulting in no significant difference in abacavir accumulation between wild-type and MDR1 (Figure 4). The Bcrp1 inhibitors Ko143 (200 nM) and FTC (10 µM) had no significant effect on [^{3}H]-abacavir cellular accumulation in either wild-type or MDR1 transfects (Figure 5).

Directional flux across MDCKII cell monolayers

Directional flux of [^{3}H]-abacavir was determined in MDCKII wild-type and MDR1 transfects. The amount of [^{3}H]-abacavir transported, shown in femtomoles (Figure 6A; specific activity 0.6Ci/mmol) and the effective permeability (P_{eff}, Figure 6B), was significantly increased in the B-to-A direction and significantly decreased in the A-to-B direction in the MDCKII-MDR1 transfects compared to wild-type cells with an efflux ratio (ER) of 4 vs. 1.3, respectively. On the other hand, there was no difference in the flux of [^{14}C]-AZT between the wild-type and MDR1 cells, where the ER values were 1.3 for the wild-type and 1.4 for the MDR1 cells (Figure 6C and 6D). For abacavir, treatment of the MDR1monolayers with the inhibitors LY335979 (1μM) and GF120918 (5μM) completely reversed the directionality of transport due to P-gp (Figure 7A-D), such that the P_{eff} in the A-to-B and B-to-A direction were not different and the ER was 1. Treatment of the MDR1-transfecetd cells with the Bcrp1 inhibitor Ko143 had no effect on abacavir transport in the A-to-B or B-to-A direction (ER of 3 in MDR1 control vs. 3.6 with Ko143 treatment, see Figure 8).

LY335979 dose dependent inhibitory effect

The P_{eff} B-to-A of abacavir across the MDCKII-MDR1 monolayer in the absence of LY335979, i.e., the maximum observable permeability (E_o), was 13E-06 cm/s (Figure 9). The concentration of LY335979 that decreased the P_{eff} B-to-A by 50% (IC_{50}) was 0.07 μM. The P_{eff} value at the highest inhibitor concentration of 1 μM ($E_o - I_{max}$) was 8E-06 cm/s. The maximal effect of LY335979 on P-gp mediated abacavir P_{eff} was given by the I_{max}, which was 5E-06 cm/s. The shape factor γ from the fit of the model to the data was 5.

DMD Fast Forward. Published on August 20, 2007 as DOI: 10.1124/dmd.107.017723
This article has not been copyedited and formatted. The final version may differ from this version.

Brain distribution of abacavir in wild-type and mdr1a (-/-) mutant CF-1 mice

The abacavir plasma and brain profiles following an intravenous bolus dose were determined in wild-type CF-1 and naturally mutant mdr1a (-/-) deficient CF-1 mice. In wild-type mice, the plasma concentrations were significantly higher than those in the brain at all sampled time points (5, 10, 20, 30 and 40 min, Figure 10A) and the brain-to-plasma concentration ratio (B/P) was less than 0.3 (mean ± SD = 0.22 ±0.04) and rapidly reached distributional equilibrium within 10 min (Figure 11). In case of the mdr1a (-/-) mutant mice, the concentrations in the brain were higher than in the plasma at all time points (Figure 10B) and the brain-to-plasma ratio was greater than 2.0, except at 5min where it was 1.2 (mean ± SD = 2.1 ±0.54) which was significantly greater than the B/P ratio in the wild-type at all time points ($p<0.01$). The B/P ratio reached a distributional equilibrium slower than in the wild-type mice (Figure 11). Non-compartmental analysis of plasma and brain data gave a terminal half life of 13.9 min in the plasma and 15.7 min in the brain in the WT (see Table 1). In case of the mdr1a (-/-) mutants the half life was 20.2 min in plasma and 20.6 min in the brain. The total body clearance in wild-type mice was 171 mL/min/kg and decreased to 91 mL/min/kg in the mutant mice. The volume of distribution at steady state, based on the plasma concentration-time profiles, was 3.1 L/kg and 2.4 L/kg in the wild-type and P-gp mutant mice, respectively. In the WT CF-1 mouse the AUC_{plasma} was 58 ± 2.5 μg-min/mL (mean ± S.D.) and AUC_{brain} was 9.8 ± 0.6 μg-min/mL, while in the mutant mice the AUC_{plasma} was 109 ± 3.1 μg-min/mL and AUC_{brain} was 202 ± 7.2 μg-min/mL. The AUC_{plasma} in the mutants was approximately 2-fold greater than wild-type mice and the AUC_{brain} in mutants was 21-fold greater than wild-type. The ratio of the $(AUC_{brain} / AUC_{plasma})_{\textbf{wild-type}}$ was

0.17 while the $(AUC_{brain}/AUC_{plasma})$ **P-gp mutant** was significantly greater at 1.85. Given these AUC ratios, the resultant drug targeting index for the enhancement in brain exposure of abacavir in the P-gp deficient mice compared to the wild-type was equal to 11.

DISCUSSION:

The interaction of abacavir with P-glycoprotein was investigated using both in vitro and in vivo methods. Initially, the stimulation of P-gp-mediated ATPase activity indicated that there was a functional binding interaction between abacavir and P-gp in isolated P-gp over-expressing membranes. The use of an isolated system such as P-gp over-expressing membranes allowed for studying the interaction of drug with P-gp without the effect of other factors (e.g., other influx and efflux transporters, cytosolic components, etc.) that might mask an interaction. Abacavir, at a concentration of 500µM, stimulated P-gp activity to a degree that was comparable to the positive control, 20µM verapamil. The high concentration of abacavir required to generate this response may indicate a moderate interaction with P-gp. The moderate response generated by abacavir compared to verapamil could be due to its interaction at a different binding site. There is evidence that P-gp expresses multiple binding sites and abacavir may be interacting with P-gp at a low affinity binding site (Pascaud et al., 1998).

In-vitro cellular transport studies were conducted since they provide the advantage of a more complete cell-based system (Polli et al., 2001). Cellular accumulation studies of abacavir were conducted in immortalized MDCKII wild-type and the MDCKII-MDR1 cells that stably over express human P-gp. Gene expression studies using real-time PCR showed significantly higher

mRNA expression for human P-gp in the MDR1-transfects (data not shown). Vinblastine, an excellent P-gp substrate, was used as a positive control to verify the functional expression of P-gp in the MDR1-MDCKII cell line (Figure 3). The significantly lower accumulation of abacavir in the MDR1-transfects compared to wild-type suggested P-gp mediated efflux of abacavir (Figure 3). This is the first direct evidence of P-gp mediated efflux of an NRTI. By comparison, AZT was not transported by P-gp. The complete restoration of abacavir accumulation in the transfects by the specific P-gp inhibitor, LY335979 (Choo et al., 2000; Dai et al., 2003) and the dual inhibitor of P-gp and Bcrp1, GF120918 further confirmed the role of P-gp in abacavir cellular accumulation (Figure 4). The slight, but not significant increase in wild-type accumulation following treatment with inhibitors may be due to effect on endogenous P-gp in the MDCK cells.

Recently, AZT and abacavir have been shown to be substrates for the drug efflux transporter Bcrp1 (Wang et al., 2003; Pan et al., 2007). Thus, the possibility that endogenous Bcrp1 might confound the results observed in the P-gp cell model was investigated. Ko143 and FTC, both selective inhibitors of Bcrp1, had no effect on the accumulation of abacavir in the MDR1 cell monolayers (Figure 5). These data indicate that there was no Bcrp1-mediated component to the active efflux of abacavir from these cells.

The effective permeability (P_{eff}) of abacavir across the MDCKII cell monolayer was measured in the wild-type and MDR1-transfects. Using tracer amounts of a radiolabeled compound, the flux study allows for detection of the existence of directionality across a cell monolayer. Knowledge of the apical membrane localization of P-gp predicts that P-gp mediated flux in the B-to-A

direction will be much greater than in the A-to-B direction. In the MDCKII-MDR1 cells there was increased directionality of abacavir flux compared to the wild-type cells (Figure 6A) and the efflux ratio was approximately 4 (Figure 6B) compared to 1.3 in the wild-type. The efflux ratio for AZT was not different between the wild-type (1.3) and MDR1-transfects (1.4). The $P_{eff\ \mathbf{B\text{-}to\text{-}A}}$ was greater than the $P_{eff\ \mathbf{A\text{-}to\text{-}B}}$ in both cell lines indicating the possible role of a common transporter that is responsible for efflux (Figure 6C, D). AZT has been shown to be effluxed by a probenecid-sensitive transporter and the baseline efflux seen in this study is possibly mediated by such a transporter (Wang et al., 1997). Moreover, over-expression of P-gp in the MDR1 cells had no effect on either the A-to-B or the B-to-A flux of AZT, indicating a lack of P-gp mediated efflux. Further evidence of P-gp mediated flux was provided by treatment of the MDR1 monolayers with LY335979 (1μM) and GF120918 (5μM) which completely abolished the directionality of abacavir transport (Figure 7A, C) and reduced the efflux ratio to unity (Figure 7B, D). Also, the Bcrp1 inhibitor Ko143 had no significant effect on P_{eff} or the efflux ratio (Figure 8A, B). These observations indicate that LY335979 and GF120918 were able to completely inhibit P-gp efflux of abacavir. The $P_{eff\ \mathbf{B\text{-}to\text{-}A}}$ of [^{3}H]-abacavir in the MDR1 monolayers was not affected by addition of up to a 1000 μM of cold abacavir in a competition assay (data not shown). This would suggest a passive process or a high-capacity influx system for abacavir uptake and a relatively high capacity related to the P-gp mediated efflux. This observation is in agreement with previous studies where the brain uptake of [^{14}C]-abacavir, following *in situ* brain perfusion in the guinea pig, was not affected by up to 200 μM cold abacavir (Thomas et al., 2001). The dose dependent inhibition of P-gp mediated B-to-A flux by LY335979 (Figure 9), in the MDR1 monolayers (Figure 7B), reduced the effective B-to-A permeability by 40% and generated an IC_{50} of 0.07μM LY335979 which was in excellent

agreement with the previously reported IC_{50} (59 nM) for LY335979-mediated inhibition of P-gp in an *in vitro* cell system (Dantzig et al., 1996).

It has been reported that abacavir can distribute to the CSF (Daluge et al., 1997; McDowell et al., 1999) but at levels significantly lower than plasma. Capparelli et al. suggested that the CSF penetration of abacavir might be sufficient to prevent viral replication of the HIV1 virus (Capparelli et al., 2005). This is contradicted by evidence of the development of different genotypic viral mutations in the brain compared to plasma, indicating discordant viral evolution (McCoig et al., 2002) and lack of viral inhibition in the brain (Kandanearatchi et al., 2004) under abacavir therapy. This is of particular concern in the case of AIDS dementia complex which is a continuing problem even with the advent of ART (Smit et al., 2004). Therefore, the role of P-gp in the brain distribution of abacavir was evaluated *in vivo* using the CF1 mouse model.

The mdr1a (-/-) CF1 mouse model is a sub-population naturally deficient in the expression of the murine mdr1a gene product, due to the loss of exon 23 during mRNA splicing (Pippert and Umbenhauer, 2001). These mutant mice lack functional P-gp in tissues such as the brain, intestine and testis (Umbenhauer et al., 1997) and are thus useful in understanding the role of P-gp in limiting CNS distribution (Kwei et al., 1999). Following intravenous administration, the B/P concentration ratio in mdr1a (+/+) CF1 wild-type mice (P-gp competent), demonstrated poor penetration of abacavir into the brain (Figure 10 A, 11). This is consistent with previously reported brain distribution of abacavir in various animal models (Daluge et al., 1997; Thomas et al., 2001) such as the guinea pig, rats and monkeys. Compared to the wild-type mice the mdr1a (-/-) mutants showed significantly enhanced brain distribution with a B/P ratio of up to 2.5 (40

min). This increase in brain distribution became even more remarkable when the B/P ratios in the mutants were compared to the wild-type, which showed up to a 10-fold increase in brain levels normalized to plasma (Figure 11).

In the wild-type mouse the plasma clearance of abacavir was high (171 ml/min/kg) and this resulted in the short plasma half-life of about 14 mins. Abacavir is a pro-drug and is rapidly converted to its active form carbovir triphosphate intracellularly in addition to being metabolized in the liver and these processes could account for the large clearance observed. The decreased plasma clearance in the mutants (91 ml/min/kg) resulted in the doubling of the AUC_{plasma} and may be due to the absence of P-gp at the liver in these animals (Pereira de Oliveira et al., 2005) resulting in loss of active efflux. It is also possible that the two-fold increase in plasma AUC in the mutants could be due to a difference in the metabolism of abacavir, even though general hepatic metabolic activity has been shown to be identical in these sub-populations (Kwei et al., 1999).

A two-fold increase in the plasma exposure in the mutant does not explain the 21-fold increase in the brain exposure reflected by the AUC_{brain}. The absence of P-gp at the BBB appears to be a critical factor determining the brain uptake of abacavir. P-gp function at the brain would impart an additional clearance out of the brain in the wild-type mice resulting in a more rapid approach to equilibrium (shorter mean transit time in the brain) than would be seen with only passive clearance (Hammarlund-Udenaes et al., 1997). Figure 11 demonstrates this phenomenon where the B/P ratio in the mutants took longer to reach equilibrium than the wild-type mice. Increased brain penetration might also lead to higher intracellular levels of abacavir resulting in the brain

levels being higher than in plasma. The AUC ratio (1.85) seen in the mutants and the drug targeting index to the brain being greater than 10 strongly suggests that P-gp expression plays a significant role in limiting the brain distribution of abacavir. Altered brain metabolism of abacavir increasing brain levels in the mutant is unlikely due to the negligible activity of alcohol dehydrogenase, the enzyme that metabolizes abacavir in conjunction with glucuronyl transferase in the liver (Zimatkin et al., 2006).

The efflux transport of NRTIs out of the brain has previously been reported for AZT and ddI (Wang and Sawchuk, 1995) by a probenecid-sensitive system (Wang et al., 1997) probably mediated by an organic anion efflux system different from any nucleoside transporter. A recent study reported high levels of Bcrp1 at the BBB and upregulation of Bcrp1 expression in the CF1 (mdr1a (-/-)) mutant mouse (Cisternino et al., 2004). In conjunction with the recent report of abacavir being a Bcrp1 substrate *in vitro* (Pan et al., 2007), this suggests that P-gp might have even a larger impact on abacavir brain distribution than observed in this study. It has been well established that P-gp is expressed in lymphocytes and can limit the entry of anti-HIV1 agents into this important site of action (Jorajuria et al., 2004). There have also been reports of increased expression of P-gp following treatment with anti-HIV agents (Ford et al., 2003). Thus, inhibition of P-gp, not only at the blood-brain barrier but also at other sites of P-gp action that are important in anti-HIV1 therapy, might improve the distribution of drug to these restricted sites and lead to inhibition of viral resistance. This study shows, both in vitro and in vivo, that P-gp is involved in the active efflux of abacavir and significant therapeutic advantage might be gained by influencing the active transport of abacavir at critical sites.

Acknowledgements

We thank Dr. Alfred H. Schinkel from Netherlands Cancer Institute for generously providing Ko143, Eli Lilly and Company for kindly providing us with LY335979, GlaxoSmithKline for kindly providing us with GF120918 and the National Cancer Institute for providing us with FTC.

References

Allen JD, van Loevezijn A, Lakhai JM, van der Valk M, van Tellingen O, Reid G, Schellens JH, Koomen GJ and Schinkel AH (2002) Potent and specific inhibition of the breast cancer resistance protein multidrug transporter in vitro and in mouse intestine by a novel analogue of fumitremorgin C. *Mol Cancer Ther* **1:**417-425.

Ances BM and Ellis RJ (2007) Dementia and neurocognitive disorders due to HIV-1 infection. *Semin Neurol* **27:**86-92.

Capparelli EV, Letendre SL, Ellis RJ, Patel P, Holland D and McCutchan JA (2005) Population pharmacokinetics of abacavir in plasma and cerebrospinal fluid. *Antimicrob Agents Chemother* **49:**2504-2506.

Choo EF, Leake B, Wandel C, Imamura H, Wood AJ, Wilkinson GR and Kim RB (2000) Pharmacological inhibition of P-glycoprotein transport enhances the distribution of HIV-1 protease inhibitors into brain and testes. *Drug Metab Dispos* **28:**655-660.

Cisternino S, Mercier C, Bourasset F, Roux F and Scherrmann JM (2004) Expression, up-regulation, and transport activity of the multidrug-resistance protein Abcg2 at the mouse blood-brain barrier. *Cancer Res* **64:**3296-3301.

Cordon-Cardo C, O'Brien JP, Casals D, Rittman-Grauer L, Biedler JL, Melamed MR and Bertino JR (1989) Multidrug-resistance gene (P-glycoprotein) is expressed by endothelial cells at blood-brain barrier sites. *Proc Natl Acad Sci U S A* **86:**695-698.

Dai H, Marbach P, Lemaire M, Hayes M and Elmquist WF (2003) Distribution of STI-571 to the brain is limited by P-glycoprotein-mediated efflux. *J Pharmacol Exp Ther* **304:**1085-1092.

Daluge SM, Good SS, Faletto MB, Miller WH, St Clair MH, Boone LR, Tisdale M, Parry NR, Reardon JE, Dornsife RE, Averett DR and Krenitsky TA (1997) 1592U89, a novel carbocyclic nucleoside analog with potent, selective anti-human immunodeficiency virus activity. *Antimicrob Agents Chemother* **41:**1082-1093.

Dantzig AH, Shepard RL, Cao J, Law KL, Ehlhardt WJ, Baughman TM, Bumol TF and Starling JJ (1996) Reversal of P-glycoprotein-mediated multidrug resistance by a potent cyclopropyldibenzosuberane modulator, LY335979. *Cancer Res* **56:**4171-4179.

Ford J, Meaden ER, Hoggard PG, Dalton M, Newton P, Williams I, Khoo SH and Back DJ (2003) Effect of protease inhibitor-containing regimens on lymphocyte multidrug resistance transporter expression. *J Antimicrob Chemother* **52:**354-358.

Fromm MF (2003) Importance of P-glycoprotein for drug disposition in humans. *Eur J Clin Invest* **33 Suppl 2:**6-9.

Hammarlund-Udenaes M, Paalzow LK and de Lange EC (1997) Drug equilibration across the blood-brain barrier--pharmacokinetic considerations based on the microdialysis method. *Pharm Res* **14:**128-134.

Jorajuria S, Dereuddre-Bosquet N, Becher F, Martin S, Porcheray F, Garrigues A, Mabondzo A, Benech H, Grassi J, Orlowski S, Dormont D and Clayette P (2004) ATP binding cassette multidrug transporters limit the anti-HIV activity of zidovudine and indinavir in infected human macrophages. *Antivir Ther* **9:**519-528.

Josephson F, Albert J, Flamholc L, Gisslen M, Karlstrom O, Lindgren SR, Naver L, Sandstrom E, Svedhem-Johansson V, Svennerholm B and Sonnerborg A (2007) Antiretroviral treatment of HIV infection: Swedish recommendations 2007. *Scand J Infect Dis* **39:**486-507.

Kandanearatchi A, Vyakarnam A, Landau S and Everall IP (2004) Suppression of human immunodeficiency virus replication in human brain tissue by nucleoside reverse transcriptase inhibitors. *J Neurovirol* **10:**136-139.

Kerza-Kwiatecki AP and Amini S (1999) CNS as an HIV-1 reservoir; BBB and drug delivery. *J Neurovirol* **5:**113-114.

Kim RB, Fromm MF, Wandel C, Leake B, Wood AJ, Roden DM and Wilkinson GR (1998) The drug transporter P-glycoprotein limits oral absorption and brain entry of HIV-1 protease inhibitors. *J Clin Invest* **101:**289-294.

Kwei GY, Alvaro RF, Chen Q, Jenkins HJ, Hop CE, Keohane CA, Ly VT, Strauss JR, Wang RW, Wang Z, Pippert TR and Umbenhauer DR (1999) Disposition of ivermectin and cyclosporin A in CF-1 mice deficient in mdr1a P-glycoprotein. *Drug Metab Dispos* **27:**581-587.

Langford D, Marquie-Beck J, de Almeida S, Lazzaretto D, Letendre S, Grant I, McCutchan JA, Masliah E and Ellis RJ (2006) Relationship of antiretroviral treatment to postmortem brain tissue viral load in human immunodeficiency virus-infected patients. *J Neurovirol* **12:**100-107.

Lipniacki A (2003) Drug resistance as the primary cause of theraupetic failures in HIV.AIDS. *HIV AIDS Rev* **2:**2-7.

McCoig C, Castrejon MM, Castano E, De Suman O, Baez C, Redondo W, McClernon D, Danehower S, Lanier ER, Richardson C, Keller A, Hetherington S, Saez-Llorens X and Ramilo O (2002) Effect of combination antiretroviral therapy on cerebrospinal fluid HIV RNA, HIV resistance, and clinical manifestations of encephalopathy. *J Pediatr* **141:**36-44.

McDowell JA, Chittick GE, Ravitch JR, Polk RE, Kerkering TM and Stein DS (1999) Pharmacokinetics of [(14)C]abacavir, a human immunodeficiency virus type 1 (HIV-1) reverse transcriptase inhibitor, administered in a single oral dose to HIV-1-infected adults: a mass balance study. *Antimicrob Agents Chemother* **43:**2855-2861.

Pan G, Giri N and Elmquist WF (2007) Abcg2/Bcrp1 mediates the polarized transport of anti-retroviral nucleosides Abacavir and Zidovudine. *Drug Metab Dispos*.

Pascaud C, Garrigos M and Orlowski S (1998) Multidrug resistance transporter P-glycoprotein has distinct but interacting binding sites for cytotoxic drugs and reversing agents. *Biochem J* **333 (Pt 2):**351-358.

Pereira de Oliveira M, Garcion E, Venisse N, Benoit JP, Couet W and Olivier JC (2005) Tissue distribution of indinavir administered as solid lipid nanocapsule formulation in mdr1a (+/+) and mdr1a (-/-) CF-1 mice. *Pharm Res* **22:**1898-1905.

Pippert TR and Umbenhauer DR (2001) The subpopulation of CF-1 mice deficient in P-glycoprotein contains a murine retroviral insertion in the mdr1a gene. *J Biochem Mol Toxicol* **15:**83-89.

Polli JW, Wring SA, Humphreys JE, Huang L, Morgan JB, Webster LO and Serabjit-Singh CS (2001) Rational use of in vitro P-glycoprotein assays in drug discovery. *J Pharmacol Exp Ther* **299:**620-628.

Smit TK, Brew BJ, Tourtellotte W, Morgello S, Gelman BB and Saksena NK (2004) Independent evolution of human immunodeficiency virus (HIV) drug resistance mutations in diverse areas of the brain in HIV-infected patients, with and without dementia, on antiretroviral treatment. *J Virol* **78:**10133-10148.

Storch CH, Theile D, Lindenmaier H, Haefeli WE and Weiss J (2007) Comparison of the inhibitory activity of anti-HIV drugs on P-glycoprotein. *Biochem Pharmacol* **73:**1573-1581.

Thomas SA, Bye A and Segal MB (2001) Transport characteristics of the anti-human immunodeficiency virus nucleoside analog, abacavir, into brain and cerebrospinal fluid. *J Pharmacol Exp Ther* **298:**947-953.

Umbenhauer DR, Lankas GR, Pippert TR, Wise LD, Cartwright ME, Hall SJ and Beare CM (1997) Identification of a P-glycoprotein-deficient subpopulation in the CF-1 mouse strain using a restriction fragment length polymorphism. *Toxicol Appl Pharmacol* **146:**88-94.

Wang X, Furukawa T, Nitanda T, Okamoto M, Sugimoto Y, Akiyama S and Baba M (2003) Breast cancer resistance protein (BCRP/ABCG2) induces cellular resistance to HIV-1 nucleoside reverse transcriptase inhibitors. *Mol Pharmacol* **63:**65-72.

Wang Y and Sawchuk RJ (1995) Zidovudine transport in the rabbit brain during intravenous and intracerebroventricular infusion. *J Pharm Sci* **84:**871-876.

Wang Y, Wei Y and Sawchuk RJ (1997) Zidovudine transport within the rabbit brain during intracerebroventricular administration and the effect of probenecid. *J Pharm Sci* **86:**1484-1490.

Weiss J, Rose J, Storch CH, Ketabi-Kiyanvash N, Sauer A, Haefeli WE and Efferth T (2007) Modulation of human BCRP (ABCG2) activity by anti-HIV drugs. *J Antimicrob Chemother* **59:**238-245.

Yuan J (1993) Estimation of variance for AUC in animal studies. *J Pharm Sci* **82:**761-763.

Zimatkin SM, Pronko SP, Vasiliou V, Gonzalez FJ and Deitrich RA (2006) Enzymatic mechanisms of ethanol oxidation in the brain. *Alcohol Clin Exp Res* **30:**1500-1505.

DMD Fast Forward. Published on August 20, 2007 as DOI: 10.1124/dmd.107.017723
This article has not been copyedited and formatted. The final version may differ from this version.

Footnotes

This project was supported by NIH grant NS42549.

Request for reprints may be addressed to:

William F. Elmquist, Ph.D.,

Department of Pharmaceutics, University of Minnesota,

308 Harvard Street SE, Weaver-Densford Hall 9-127,

Minneapolis, Minnesota, USA 55455

e-mail: elmqu011@umn.edu

DMD Fast Forward. Published on August 20, 2007 as DOI: 10.1124/dmd.107.017723
This article has not been copyedited and formatted. The final version may differ from this version.

Legends

Figure 1 Structures of the nucleoside analogs Abacavir and Zidovudine (AZT), P-gp inhibitors (LY335979 and GF120918) and the BCRP inhibitors (Ko143, FTC)

Figure 2 Stimulation of P-gp ATPase activity by abacavir. The ATPase activity expressed as nanomoles of phosphate generated/ mg protein/min was significantly stimulated by 500 µM of abacavir (**, $p<0.01$) over control P-gp membranes. The positive control verapamil (20µM) also significantly stimulated P-gp ATPase activity (**, $p<0.01$); n= 3-7.

Figure 3 Accumulation of [^{3}H]-abacavir, [^{3}H]-vinblastine (positive control) and [^{14}C]-AZT in wild-type (■) and MDR1-transfected (▭) MDCK cells. Results are expressed as mean ± S.D. (as percentage of wild-type control); n= 6-18 (***, $p<0.001$, compared with wild-type control group). Significantly lower accumulation of abacavir and vinblastine in the MDR1 cells but no statistical difference for AZT accumulation between wild-type and MDCKII-MDR1 cells.

Figure 4 Accumulation of [^{3}H]-abacavir in wild-type (■) and MDR1-transfected (▭) MDCK cells and the effect of the P-gp inhibitors LY335979 (1µM) and GF120918 (5 µM). Results are expressed as mean ± S.D. (as percentage of wild-type control); n=9 (**, $p<0.01$, compared with wild-type control group; ††, $p<0.01$, compared to MDR1 control group). [^{3}H]-vinblastine (n=6) was used as a positive control for P-gp function. Both the inhibitors restored abacavir level in the MDR1 cells such that it was not different from wild-type control)

DMD Fast Forward. Published on August 20, 2007 as DOI: 10.1124/dmd.107.017723
This article has not been copyedited and formatted. The final version may differ from this version.

Figure 5 Accumulation of [^{3}H]-abacavir in wild-type (■) and MDR1-transfected (▭) MDCK cells and the effect of the Bcrp1 inhibitors Ko143 (200nM) and FTC (10µM). Results are expressed as mean ± S.D. (as percentage of wild-type control); n=3-6 (**, $p<0.01$, compared with wild-type control group). There was no effect of Bcrp1 inhibitors on the cell accumulation of abacavir in MDCKII-MDR1 cells.

Figure 6 Directional flux of [^{3}H]-abacavir **(6A, B)** and [^{3}H]-AZT **(6C, D)** across the MDCKII monolayers in wild-type (●, A-to-B transport; ○, B-to-A transport) and MDR1-transfected cells (▼, A-to-B transport; Δ, B-to-A transport). Effective permeability (P_{eff}) for [^{3}H]-abacavir and [^{3}H]-AZT transport **(6 B, D)** across wild-type and MDR1 monolayers (black bars: A-to-B direction, grey bars: B-to-A direction). Results are expressed as mean ± S.D. (n=3) (***, $p<0.001$, compared to wild-type control). Increase in the P_{eff} and amount transported B-to-A and decrease in the P_{eff} and amount transported A-to-B was seen for abacavir in the MDR1 monolayers compared to wild-type cells. No difference in P_{eff} was observed between wild-type and MDR1 cells for AZT.

Figure 7 Directional flux of [^{3}H]-abacavir across the MDCKII -MDR1-transfected cell monolayers in the absence (●, A-to-B transport; ○, B-to-A transport) and presence (▼, A-to-B transport; Δ, B-to-A transport) of P-gp inhibitors **(A)** LY335979 (1µM) and **(C)** GF120918 (5 µM). Arrows indicate the effect of inhibitor on flux in both directions. Effect of the P-gp inhibitors **(B)** LY335979 (1µM) and the dual (P-gp and Bcrp1) inhibitor **(D)** GF120918 (5 µM) on the effective permeability (P_{eff}) of [^{3}H]-abacavir. In the presence of inhibitors, the P_{eff} was significantly increased in the A-to-B direction (black bars) and significantly decreased in the B-

to-A direction (grey bars). Results are expressed as mean ± S.D. (n=9) (**, $p<0.01$, compared to MDR1 control)

Figure 8 (A) Directional flux of [^{3}H]-abacavir across the MDCKII -MDR1-transfected cell monolayers in the absence (●, A-to-B transport; ○, B-to-A transport) and presence (▼, A-to-B transport; Δ, B-to-A transport) of the Bcrp1 inhibitor Ko143. **(B)** Effect of the Bcrp1 inhibitor Ko143 (200nM) on the effective permeability (P_{eff}) of [^{3}H]-abacavir. There was no significant effect of Ko143 on the P_{eff} in the A-to-B direction (black bars) or B-to-A direction (grey bars) and the B-to-A P_{eff} was significantly greater than the A-to-B P_{eff} in both the Ko143 treated and control cases. **, $p<0.01$, n=3-6. Results are expressed as mean ± S.D.

Figure 9 Effect of the increasing concentration of the P-gp inhibitor LY335979 (μM) on the B-to-A P_{eff} (cm/s) of abacavir. An inhibitory E_{max} model with baseline effect was fit to the data. LY335979 inhibited the P-gp mediated B-to-A flux by 50% (IC_{50}) at 0.07 μM. ●, observed B-to-A P_{eff} values; solid line, predicted P_{eff} values from the model; □---, P_{eff} value for control case where no inhibitor was used. n= 3-9.

Figure 10 Brian distribution of abacavir in the mdr1a (-/-) deficient and wild-type CF-1 mouse following intravenous dosing. Mdr1a (-/-) and wild-type (mdr1a (+/+)) mice received 10mg/kg abacavir via tail vein injection. The brain and plasma samples were collected post- dose (5, 10, 20, 30 and 40 mins; n=6), the samples analyzed by HPLC and plotted on rectangular coordinates. **(A)** Concentration time profiles of abacavir in plasma (◊; solid line) and brain (●; dashed line) wild-type CF1 mice. **(B)** Concentration time profiles in plasma and brain of naturally mutant mdr1a (-/-) deficient CF1 mice. The brain concentrations in the mdr1a (-/-) CF1 mutant mice were significantly higher than the in the wild-type mice. Data represented as mean ± S.D.

Figure 11 Comparison of the brain to plasma concentration ratios (C_b/C_p) between wild-type CF-1 (◊) and mutant mdr1a (-/-) deficient CF-1 (●) at different sampling time points. The (C_b/C_p) ratio for ABC in the mdr1a (-/-) deficient CF1 mutants was significantly greater than the (C_b/C_p) ratio in the wild-type mice at all time points, (**; $p< 0.01$, n=5-6 per time point). Results are expressed as mean ± S.D.

DMD Fast Forward. Published on August 20, 2007 as DOI: 10.1124/dmd.107.017723
This article has not been copyedited and formatted. The final version may differ from this version.

Table 1. Plasma and brain pharmacokinetic parameters determined by non-compartmental analysis following the administration of a single I.V bolus dose of abacavir in wild-type CF1 and mdr1a (-/-) mutant CF1 mice. The AUC is expressed as mean ± S.D.

	Wild-type CF1 mouse		**mdr1a(-/-) CF1 mouse**	
Pharmacokinetic parameters	**Plasma**	**Brain**	**Plasma**	**Brain**
λz (min^{-1})	0.05	0.04	0.03	0.03
Half-life (mins)	13.9	15.7	20.2	20.6
Clearance (mL/min/kg)	171	-	91	-
Volume of distribution (L/kg)	3.15	-	2.40	-
$AUC_{(0\rightarrow inf)}$ (μg*min/mL)[a]	58±2.5	9.8±0.6	109±3.1*	202±7.2†
AUC_{brain}/AUC_{plasma}	0.17		1.85	

a *- Mean ± S.D.*

(*, $p<0.05$ for mutant vs. wild-type AUC_{plasma}; †, $p<0.05$ for mutant vs. wild-type AUC_{brain})

DMD Fast Forward. Published on August 20, 2007 as DOI: 10.1124/dmd.107.017723
This article has not been copyedited and formatted. The final version may differ from this version.

Figure 1

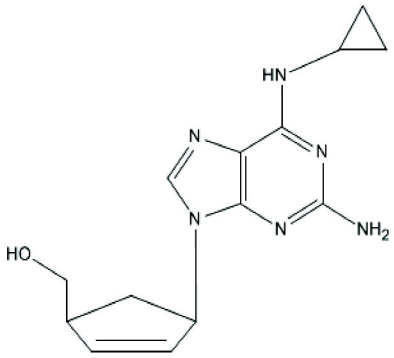

Abacavir

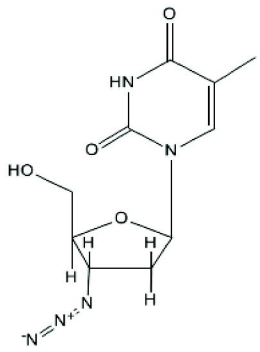

AZT

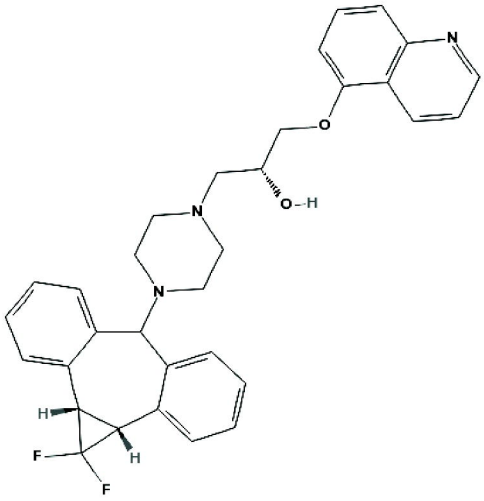

LY335979

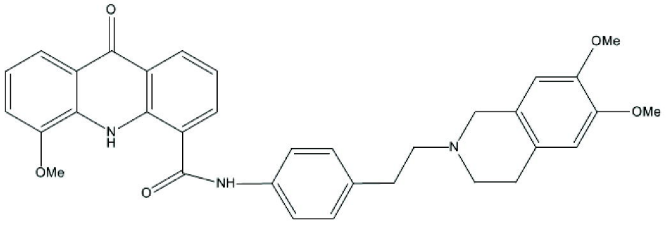

GF120918

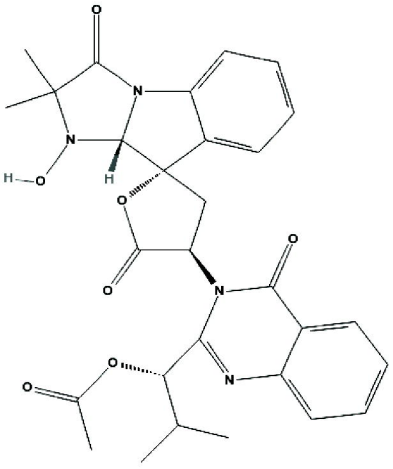

Fumitremorgin C

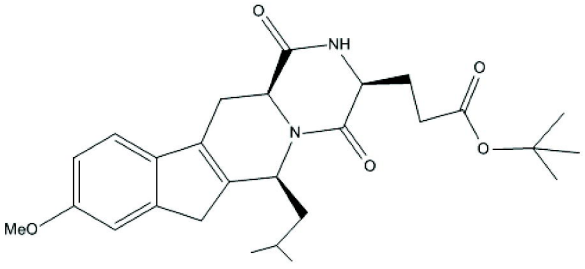

Ko143

DMD Fast Forward. Published on August 20, 2007 as DOI: 10.1124/dmd.107.017723
This article has not been copyedited and formatted. The final version may differ from this version.

Figure 2

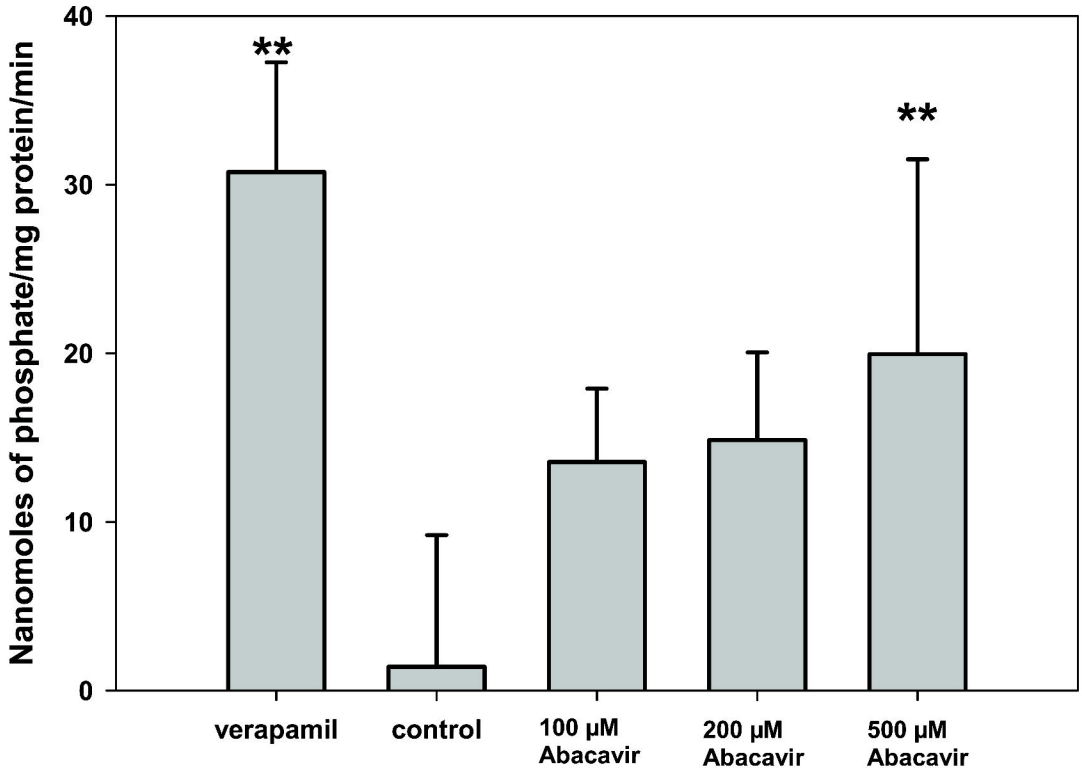

DMD Fast Forward. Published on August 20, 2007 as DOI: 10.1124/dmd.107.017723
This article has not been copyedited and formatted. The final version may differ from this version.

Figure 3

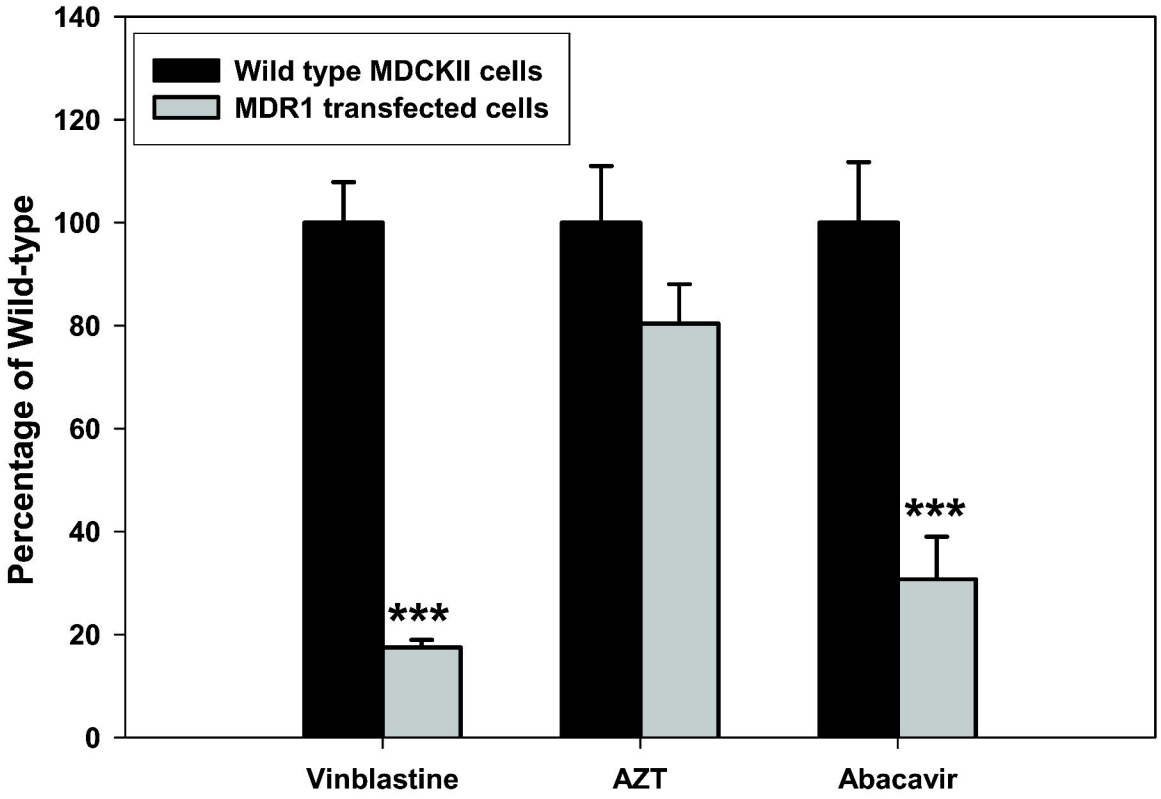

DMD Fast Forward. Published on August 20, 2007 as DOI: 10.1124/dmd.107.017723
This article has not been copyedited and formatted. The final version may differ from this version.

Figure 4

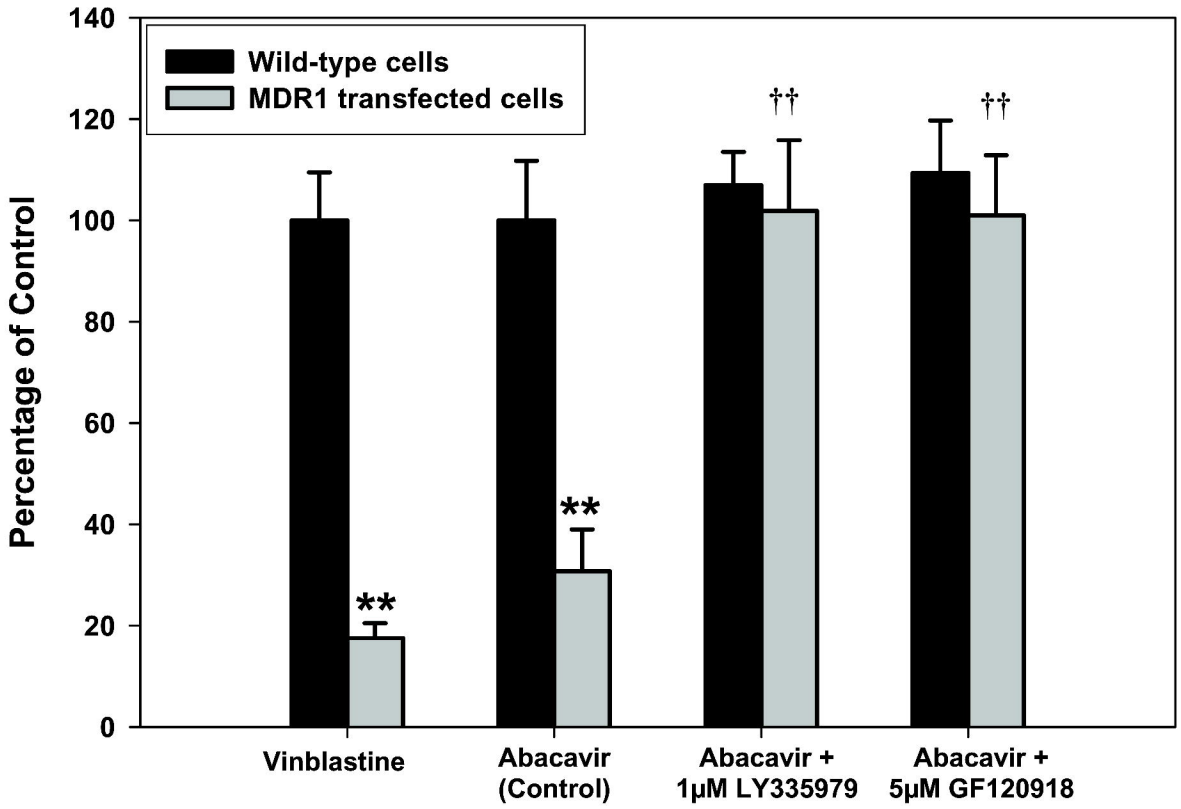

DMD Fast Forward. Published on August 20, 2007 as DOI: 10.1124/dmd.107.017723
This article has not been copyedited and formatted. The final version may differ from this version.

Figure 5

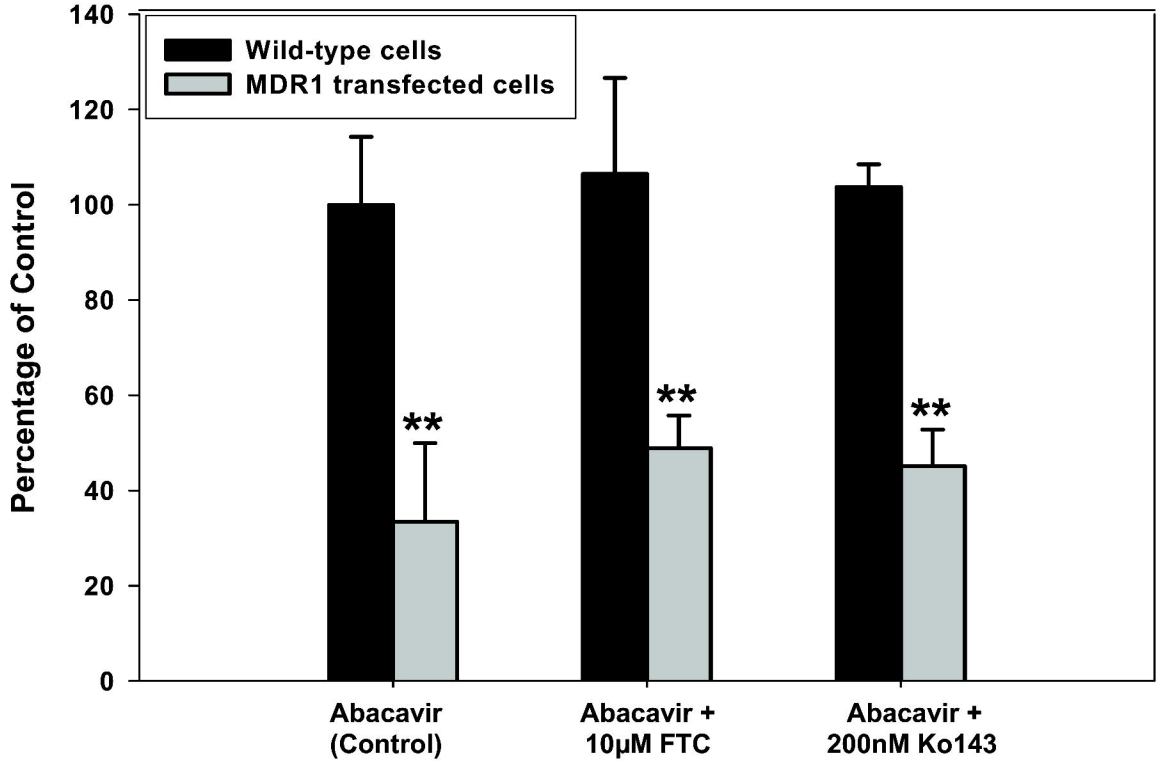

DMD Fast Forward. Published on August 20, 2007 as DOI: 10.1124/dmd.107.017723
This article has not been copyedited and formatted. The final version may differ from this version.

Figure 6

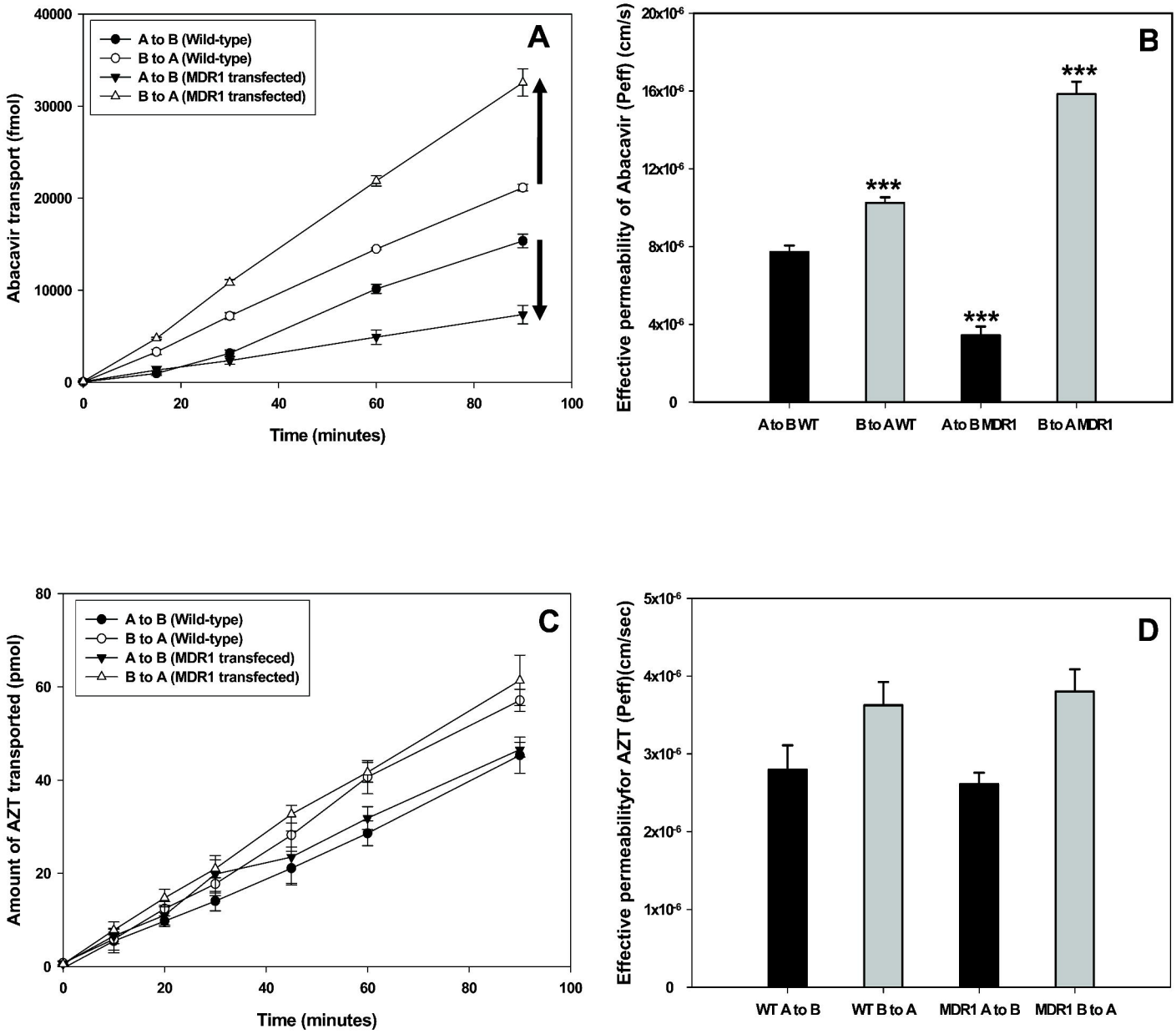

DMD Fast Forward. Published on August 20, 2007 as DOI: 10.1124/dmd.107.017723
This article has not been copyedited and formatted. The final version may differ from this version.

Figure 7

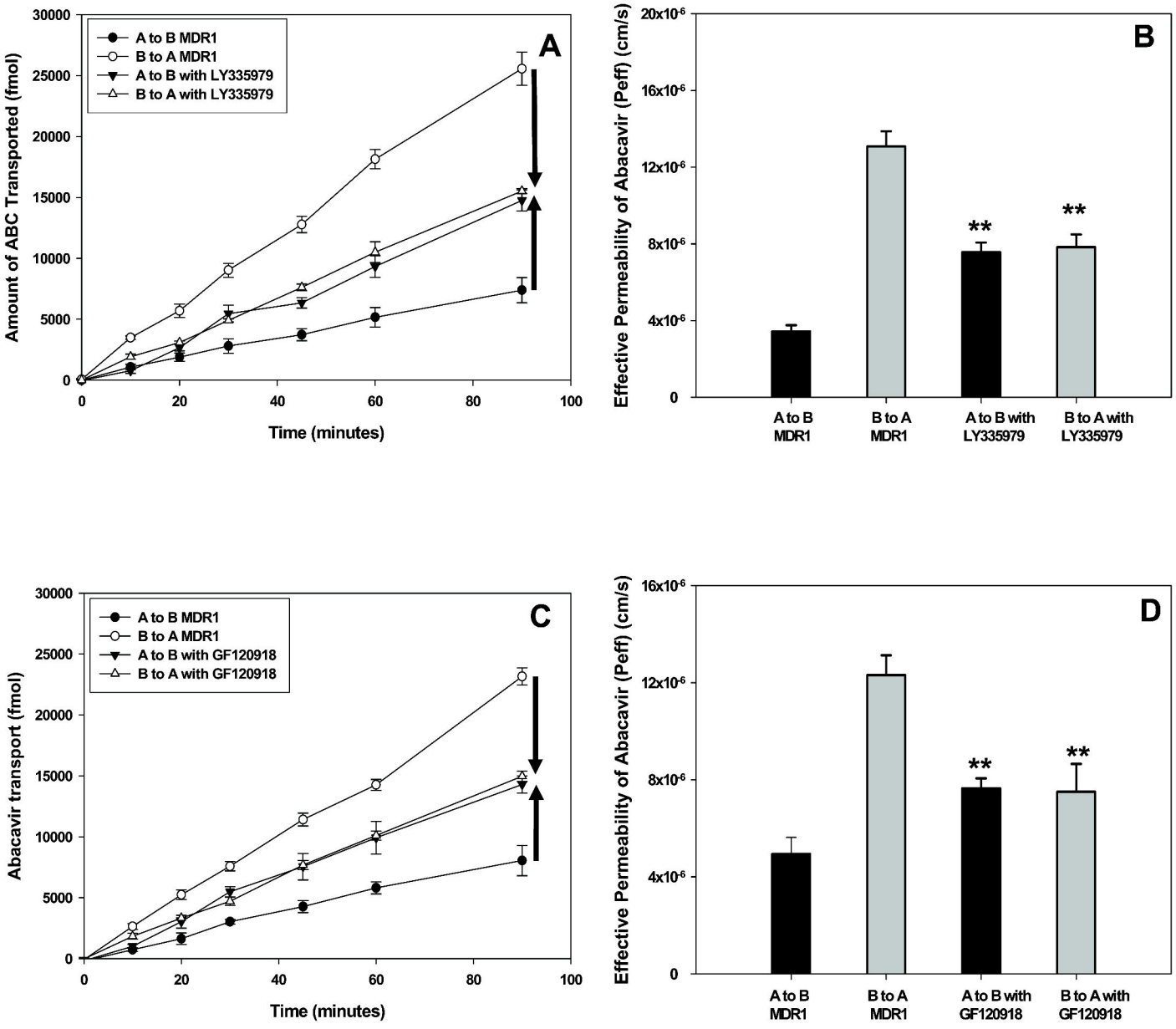

DMD Fast Forward. Published on August 20, 2007 as DOI: 10.1124/dmd.107.017723
This article has not been copyedited and formatted. The final version may differ from this version.

Figure 8

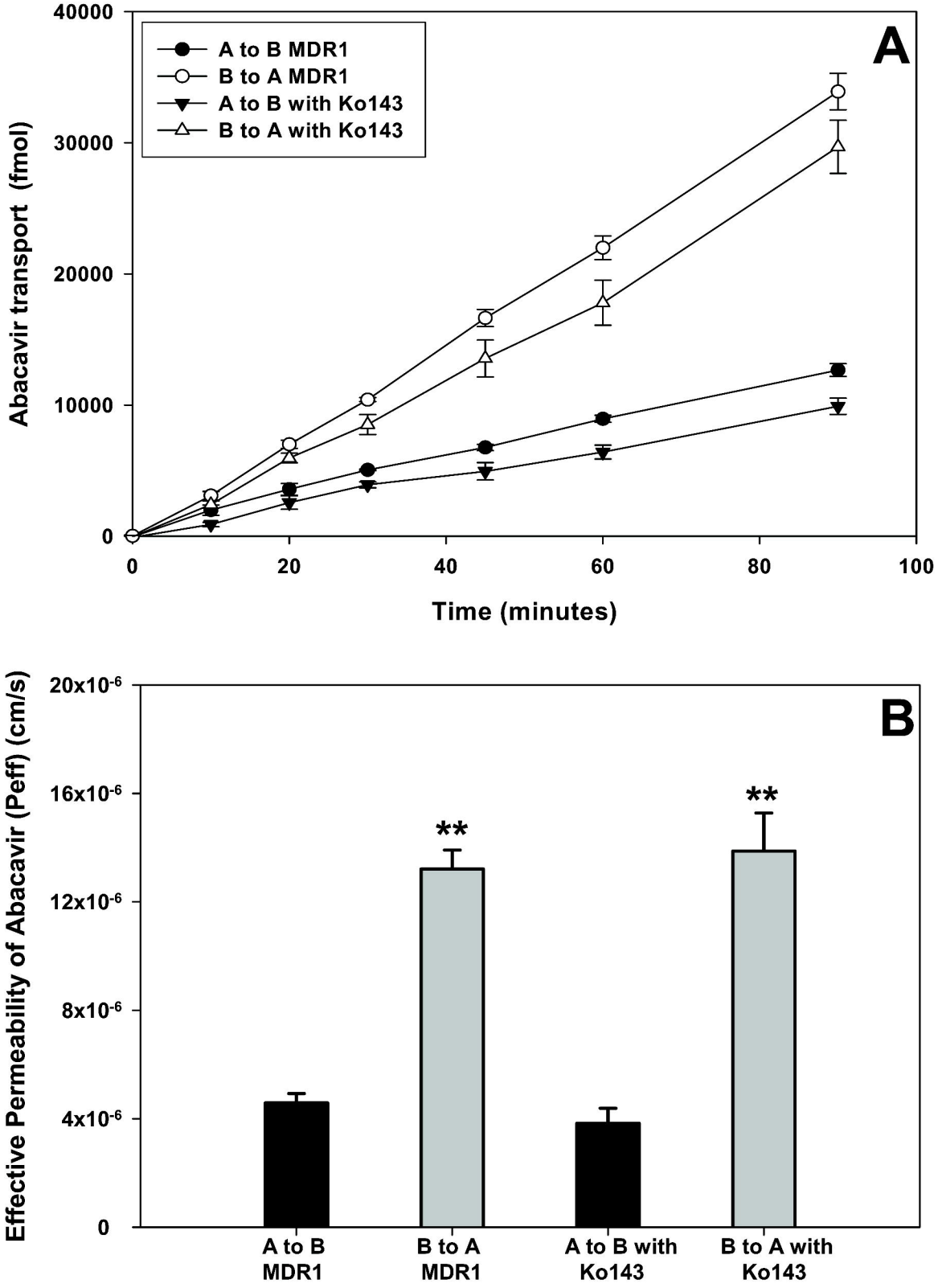

DMD Fast Forward. Published on August 20, 2007 as DOI: 10.1124/dmd.107.017723
This article has not been copyedited and formatted. The final version may differ from this version.

Figure 9

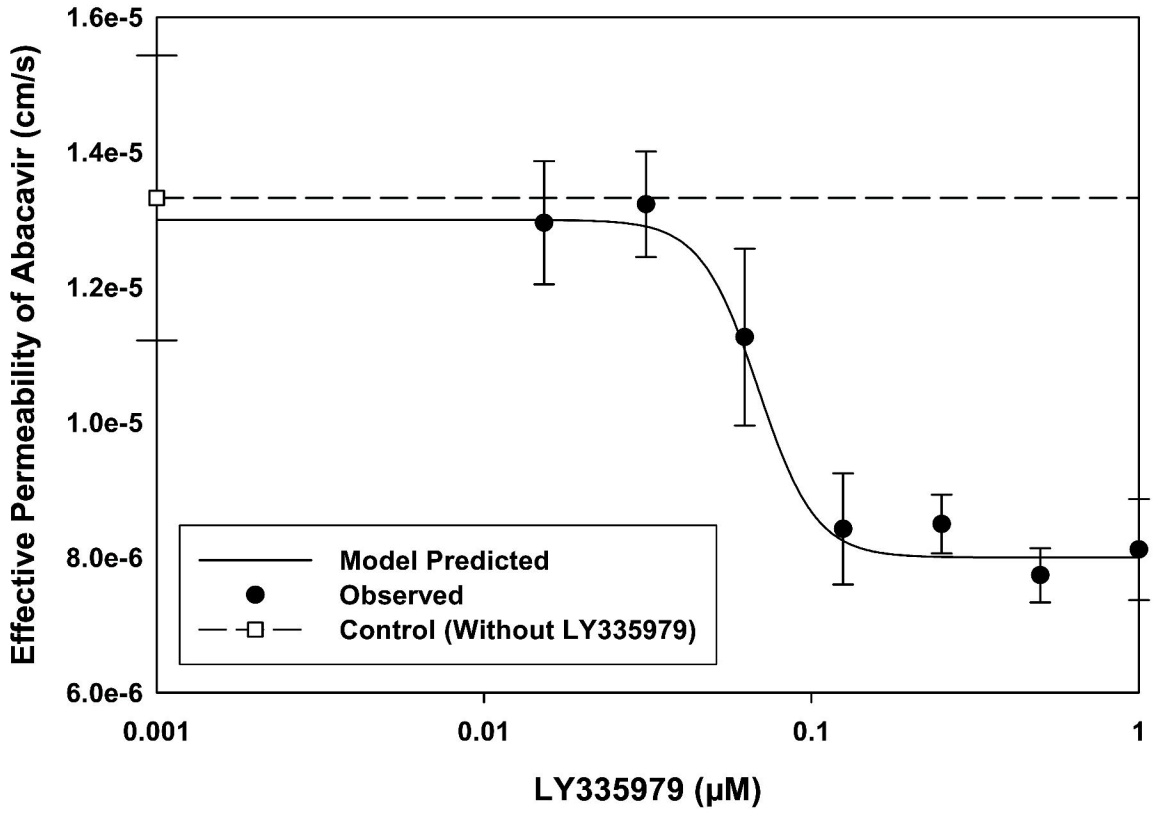

DMD Fast Forward. Published on August 20, 2007 as DOI: 10.1124/dmd.107.017723
This article has not been copyedited and formatted. The final version may differ from this version.

Figure 10

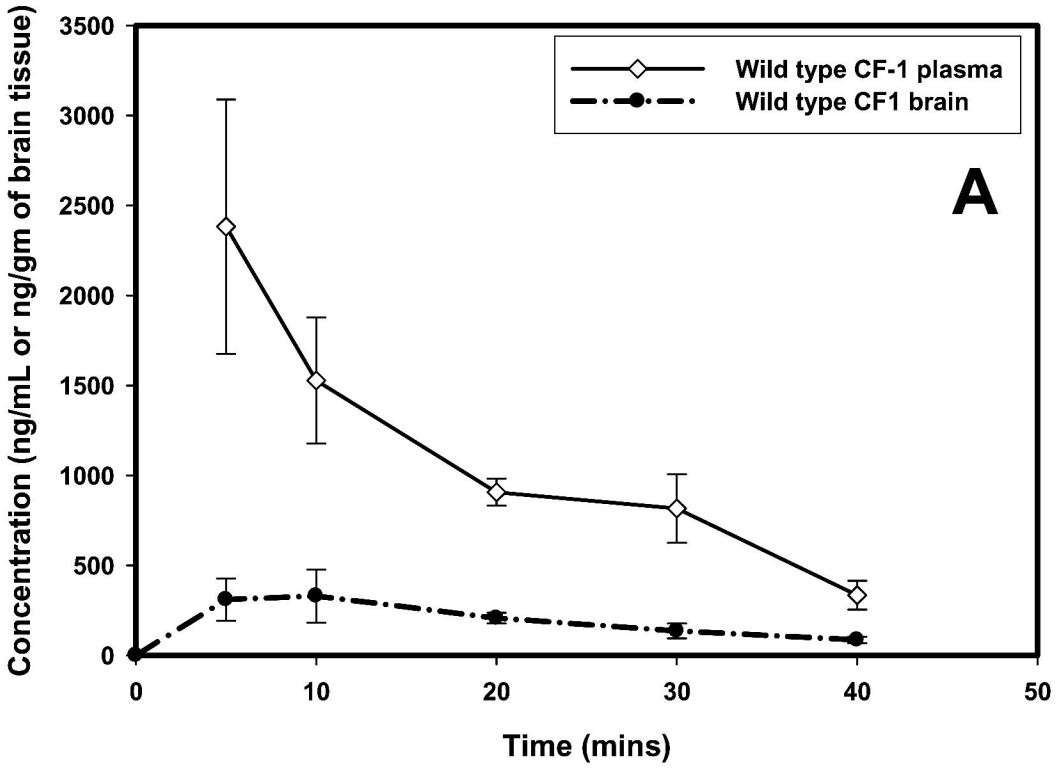

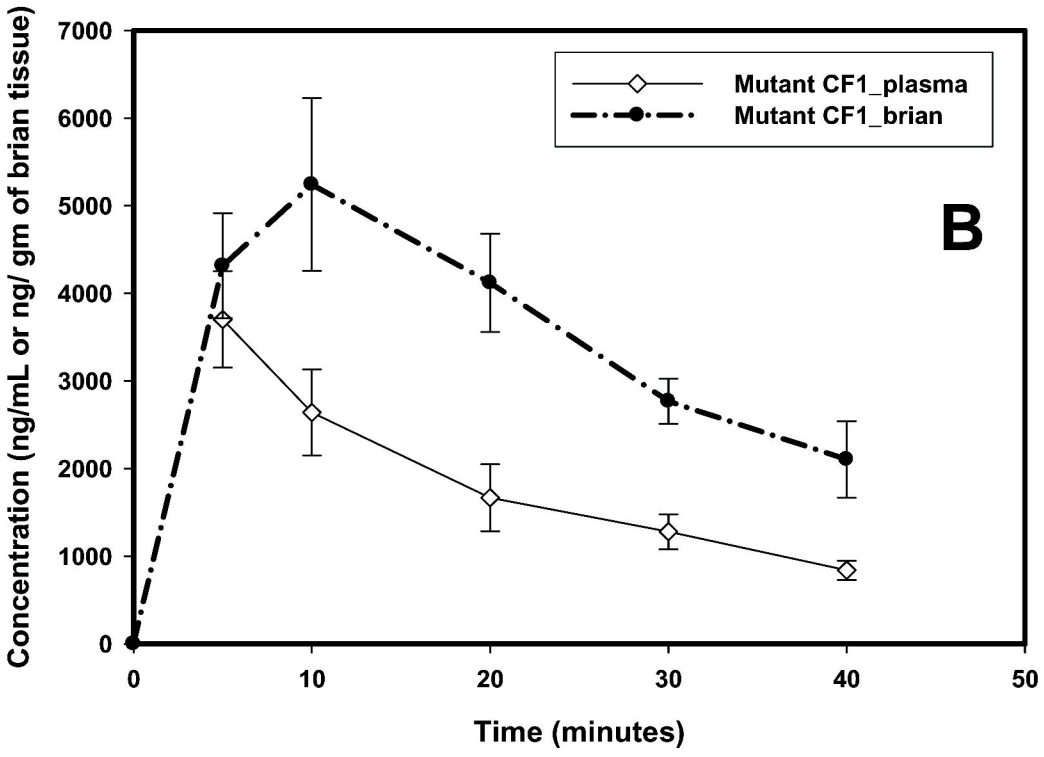

DMD Fast Forward. Published on August 20, 2007 as DOI: 10.1124/dmd.107.017723
This article has not been copyedited and formatted. The final version may differ from this version.

Figure 11